An Optimization Framework to Study the Balance Between Expected Fatalities due to COVID-19 and the Reopening of U.S. Communities

Victoria C. P. Chen, Ph.D., Yuan Zhou, Ph.D., Alireza Fallahi, Ph.D.,
Amith Viswanatha, Jingmei Yang, Yasaman Ghasemi,
Nilabh. S. Ohol, Ph.D., Ashkan A. Farahani, Ph.D., Jay M. Rosenberger, Ph.D.

Center on Stochastic Modeling, Optimization, & Statistics (COSMOS)
Department of Industrial, Manufacturing, and Systems Engineering
The University of Texas at Arlington, Arlington, TX, U.S.A.

Feng Liu, Ph.D.*

School of Systems and Enterprises
Stevens Institute of Technology, Hoboken, NJ, U.S.A.

Jeffrey B. Guild, Ph.D.

Department of Radiology
The University of Texas Southwestern Medical Center, Dallas, TX, U.S.A.

COSMOS Technical Report 20-02

*Corresponding author

Abstract

During the COVID-19 Pandemic, communities faced two conflicting objectives: (1) minimizing infections among vulnerable populations with higher risk for severe illness, and (2) enabling reopening to revive American livelihoods. The U.S. pandemic strategy myopically considered one objective at a time, with lockdowns that addressed the former, but were detrimental to the latter, and phased reopening that pursued the latter, but lost control over the former. Universal mask mandates and limitations on gatherings have yielded insufficient compliance. How could we prioritize interventions to simultaneously minimize cases of severe illness and fatalities while reopening? A team of researchers anchored by the Center on Stochastic Modeling, Optimization, & Statistics (COSMOS) at the University of Texas at Arlington has formulated a computationally-efficient optimization framework, referred to as COSMOS COVID-19 Linear Programming (CC19LP), to study the delicate balance between the expected fatality rate due to cases of severe illness and the level of normalcy in the community. The key to the CC19LP framework is a focus on "key contacts" that separate individuals at higher risk from the rest of the population. CC19LP minimizes expected fatalities by optimizing the use of available interventions, namely COVID-19 testing, personal protective equipment (PPE), recently approved COVID-19 vaccines, and social precautions, such as distancing, handwashing, and face coverings. A C3.ai award-winning online CC19LP tool is accessible from the COSMOS COVID-19 project site (https://cosmos.uta.edu/projects/covid-19/) and has been tested for all 3,142 U.S. county areas. Results are demonstrated for several metropolitan counties with a deeper investigation for Miami-Dade County in Florida.

Keywords: SARS-CoV-2, COVID-19, Optimization, Disease Modeling, Reopening

Note to Practitioners: Abstract—In this paper, a computationally fast optimization framework is presented to study the delicate balance between reopening U.S. communities and controlling severe cases of COVID-19 that lead to hospitalizations and fatalities. This framework can provide guidance to decision-makers on optimal intervention strategies for protecting high-risk individuals while reopening communities. Resources on understanding and implementing the framework are publicly available, including an award-winning online optimization tool that automatically accesses county-level data from Census, CDC, and Johns Hopkins COVID-19 repositories.

1. Introduction

Widespread transmission of the novel coronavirus, SARS-CoV-2, compromised U.S. efforts to contain the spread of the COVID-19 associated illness and subsequent fatalities. Prior guidelines to avoid the spread of viruses are based on the premise that infected individuals are most contagious after the onset of symptoms [1]. However, studies of SARS-CoV-2 have demonstrated asymptomatic and pre-symptomatic transmission [2-5], corroborated by antibody testing [6]. Recognized *social precautions* to prevent the spread of SARS-CoV-2 consist of 6-foot social distancing, personal hygiene (handwashing for at least 20 seconds with non-antibacterial soap or using hand sanitizers with at least 60% alcohol content), face coverings [7], and quarantine for infected individuals [8]. Properly maintaining social precautions means conducting *all of them*. An individual that wears a face covering, but violates social distancing is *not* properly maintaining precautions. Successful containment of the virus has been seen in countries with rigorous contact tracing combined with abundant COVID-19 testing capabilities, and public compliance with social precautions [9-10]. However, the U.S. faces issues with limited resources to implement contact tracing and the threat of non-compliance by lower-risk individuals [11-12].

The key question is: How can we achieve a low rate of severe cases while reopening communities under realistic assumptions and limited resources? Because 81% of infected individuals have mild to moderate disease [13] and may not quarantine, studies emphasize the need to isolate or shield individuals that have a higher risk of fatality [14-15]. Strategies that are applied universally are, in actuality, unfair to those at higher risk that require additional protection to equalize their risk. However, isolating high-risk groups is impractical since many need employment, require assistance, or live in environments with "crowding" and cannot isolate. In this paper, we present the COSMOS COVID-19 linear programming (CC19LP) optimization framework that enables study of the trade-off between the expected fatality rate and the normalcy of activities by "key contact" individuals in the population. Linear programming is a computationally fast and well-established methodology that has proven applicability across innumerable domains (e.g., [16-24]). Fatality rate was chosen to represent health impacts because fatalities are highly correlated with cases of severe illness, and case counts do not distinguish mild cases from severe ones. CC19LP minimizes expected fatalities by optimizing the use of *interventions*, namely social precautions, COVID-19 testing, personal protective equipment (PPE at the level of N95 respirator masks), and vaccination. Other than N95 masks, high-grade PPE can be achieved by installing protection barriers, double-masking, or combining a face shield with a mask [25-27].

Established approaches in public health for studying infectious disease outbreaks involve the use of SEIR (Susceptible-Exposed-Infectious-Recovered) models, which simulate disease transmission in a population [28-34]. These SEIR models can represent interventions, such as social distancing by reducing contact rates or vaccination by reducing transmission probabilities but cannot be directly optimized because controllable interventions are not explicitly defined. Further, these models require detailed assumptions that affect the evolution of disease transmission. For the COVID-19 Pandemic, there are varied SEIR models that attempt to simulate the progression of the pandemic because the validity of the various assumptions is

uncertain (e.g., [34]). By contrast CC19LP clearly defines controllable interventions in an aggregate framework that is deliberately parameterized to yield optimal interventions that are insensitive to uncertain information. Benchmarking is based on actual reported cases and fatalities.

2. CC19LP Model

2.1 Definition of Key Contact Individuals

The CC19LP framework was motivated by the concept of taking care of yourself, so that you can continue to care for others [35]. In this concept, the vulnerable group only stays protected if associated caregivers remain healthy. The CC19LP framework is based on partitioning the population into three non-overlapping groups, listed below and described in Figure 1. A questionnaire was developed to assist individuals in identifying their group and can be accessed from the COSMOS COVID-19 project site (https://cosmos.uta.edu/projects/covid-19/).

Group 1: *Sheltered high-risk individuals* that can isolate with the assistance of key contact individuals in Group 2.

Group 2: COVID-19 *key contacts* that simultaneously have a role in protecting high-risk individuals in Group 1 and cannot avoid interaction with the rest of the population in Group 3.

Group 3: *Baseline low-risk individuals* that do not belong to Group 2.

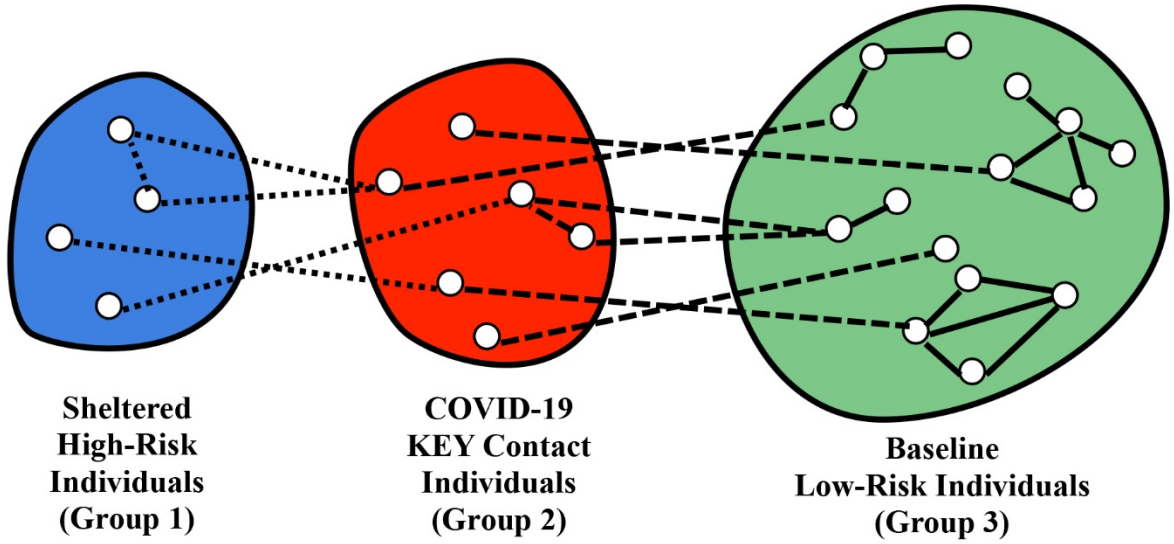

Figure 1: Partitioning the population into three non-overlapping groups. The role of Group 2 is to minimize transmission of the virus from Group 3 to Group 1. Dotted lines denote contacts with shelter-in-place. Dashed lines denote contacts requiring usage of social precautions, PPE, or testing. Solid lines denote baseline contacts without additional interventions.

The focus of CC19LP is on controlling key contacts (Group 2), which consist of those with the following characteristics:

- High-risk individuals that have an occupation, such as employment, college, or volunteer activity (including those that are seeking employment).
- High-risk individuals that reside in a crowding environment, such as lower-income communities and nursing homes.
- Workers in health care and public safety, including nursing homes and jails.
- Low-risk individuals that cannot avoid close contact with sheltered high-risk individuals.

A household with two low-risk adults, two low-risk children, and one elderly grandparent would be classified as having one sheltered high-risk individual, one low-risk adult key contact, one baseline low-risk adult, and two baseline low-risk children. Children in K-12 school can be key contacts if they cannot avoid contact with sheltered high-risk individuals in their household. Excluded from the key contact population are K-12 children that are themselves high-risk and should remain isolated. It is assumed that asymptomatic or pre-symptomatic contagious individuals still exist in the larger population and can infect key contact individuals.

Both the concepts of isolating and shielding can be incorporated in the CC19LP framework, where those that cannot avoid interaction with both the sheltered high-risk group and the baseline low-risk group should be classified as key contacts. High-risk children are among the sheltered high-risk group and will have a parent or guardian as a key contact. Low-risk younger children (aged 0-4) are in the baseline low-risk group. Recovered individuals can be key contacts or baseline low-risk individuals and are modeled in CC19LP has having immunity similar to vaccination. While compliance by key contacts may be a concern, the issue of compliance is lessened because CC19LP interventions are focused on maximizing benefit and are not applied to the entire population. The representation of social precautions is modeled as compliance in activities in the next section.

The risk types for key contact individuals explicitly distinguish those whose environment involves "crowding" that does not permit recommended social precautions, i.e., social distancing, handwashing, etc. Three risk types are defined for key contacts, as follows:

L_1 = low-risk (key) individual that can comply with social precautions,
H_1 = high-risk (key) individual that can comply with social precautions,
H_2 = high-risk (key) individual that are subject to a crowding environment.

Since high-risk children are not included among key contact individuals, only risk type L_1 can represent K-12 key contacts. The crowding characteristic for risk type H_2 will be seen later as affecting the community activity level that may be assumed of these individuals. Further, the estimation of fatalities counts sheltered high-risk individuals that are associated with key contact individuals, so as to appropriately capture the larger impact of infecting a key contact.

2.2 Community Activity Levels

Because key contact individuals must interact with the larger community, CC19LP assigns key contact individuals to allowable levels of activity. Normalcy is represented on a scale of 0 to 10 in CC19LP, where 0 mimics an environment closest to compliance with widely enforced shelter-in-place orders, and 10 mimics pre-pandemic activity without social precautions. Activity levels for key contacts define compliance with social precautions. Key contact children are assumed to participate in K-12 school, and key contact adults are assumed to participate in an occupation,

such as employment or post-secondary school or other activities during work hours. All key contacts may additionally participate in community activities. Average contact rates assumed for each level are given in parentheses and are based on the disease transmission literature for agent-based modeling [31-33].

Because online K-12 school has been largely unsuccessful [36], only in-person schooling is considered for K-12 children, at two levels:

S_1 = in-person K-12 school properly maintaining social precautions (0.10 contacts/day),

S_2 = in-person K-12 school without social precautions (4.9 contacts/day).

For some K-12 key contacts, the school level S_1 may not be possible, so the school level S_2 can be constrained with a lower limit. Because online work is a viable option for some occupations, work for adult key contacts is considered at three levels:

W_0 = online work/occupation (no contacts/day),

W_1 = in-person work/occupation properly maintaining social precautions (0.09 contacts/day),

W_2 = in-person work/occupation without social precautions (5.5 contacts/day).

The online work level W_0 can be constrained by an upper limit on the number of key contact individuals that can be employed in occupations that permit completely online participation. By contrast, the near-normal work level W_2 can be constrained by a lower limit to represent occupations, such as hospital workers, that can only be conducted in close contact with other individuals.

In addition to occupations (S or W) above, each key contact individual may participate in other community activities, specified in five levels:

A_1 = 0% of normal: all activities properly maintain social precautions (0.10 contacts/day),

A_2 = 25% of normal (1.9 contacts/day),

A_3 = 50% of normal (3.8 contacts/day),

A_4 = 75% of normal (5.7 contacts/day),

A_5 = 100% of normal: Pre-pandemic normal level (7.7 contacts/day).

An individual at activity level A_1 might choose not to participate in additional community activities, but in general can only participate in activities that permit maintaining social distancing and other precautions. To facilitate this, organizations would need to create environments that support precautions for their patrons that are key contacts. An individual at activity level A_2 might maintain precautions indoors, but outdoors plays sports with normal contacts; or might go to occasional events (e.g., theater, restaurants) without precautions, but otherwise maintains precautions. An individual at activity level A_3 maintains precautions about half the time, which is similar to the overall level of compliance among individuals aged 18-31 years [12] prior to shelter-in-place orders. An individual at activity level A_4 might frequently participate in contact activities of small to moderate size (e.g., daily gym, neighborhood gatherings) without precautions, but maintains precautions when not too inconvenient. Activity levels A_4 and A_5 in general represent more normal activities, including large gatherings (e.g., church, conferences, season passes to events) without precautions, with the difference indicating the frequency of participation in such activities. In particular, key contact risk type H_2 will have a high proportion at activity levels A_4 and A_5 to represent the crowding characteristic. A CC19LP

solution will assign key contacts to exactly one occupation level (*S* or *W*) and exactly one activity level.

To represent previously mentioned limitations on occupation and activity levels, the following fractions are defined:

$f_{S_2}^i$ = minimum fraction that canNOT comply with social precautions at K-12 school,
$f_{W_0}^i$ = maximum fraction that can do their work completely online,
$f_{W_2}^i$ = minimum fraction that canNOT comply with social precautions at work,
$f_{A_1}^i$ = maximum fraction whose activity level can satisfy A_1,
$f_{A_2}^i$ = additional maximum fraction whose activity level can satisfy A_2 or A_1,
$f_{A_5}^i$ = minimum fraction whose activity level must be A_5,
$f_{A_4}^i$ = additional minimum fraction whose activity level can be A_4 or A_5.

These fractions are input parameters to CC19LP and can be modified appropriately for different regions.

The CC19LP decision variables assign social precaution interventions, based on occupation and activity levels, to key contact individuals, both uninfected and recovered from COVID-19. In addition, decision variables can assign *transmission interventions*, namely COVID-19 swab testing, the use of PPE at the level of N95 respirator masks, and COVID-19 vaccination. Let

x_{jk}^i = # of key contacts of type *i* in required occupation *j* that have activity level *k*,
x_{jkR}^i = # of type *i* in occupation *j* that have activity level *k* and are recovered,
x_{jkT}^i = # of type *i* in occupation *j* that have activity level *k* and have COVID-19 testing,
x_{jkM}^i = # of type *i* in occupation *j* that have activity level *k* and use high-grade PPE,
x_{jkV}^i = # of type *i* in occupation *j* that have activity level *k* and are fully vaccinated,

where $i \in \{L_1, H_1, H_2\}$, $j \in \{S_1, S_2, W_0, W_1, W_2\}$, $k \in \{A_1, A_2, A_3, A_4, A_5\}$. Vaccinated individuals are represented cumulatively, where the number of individuals already vaccinated is provided as input. Note that because there are no high-risk children that are key contact individuals, for $i \in \{H_1, H_2\}$ and $j \in \{S_1, S_2\}$, $x_{jk}^i = 0$. Because of the scarceness of resources, it is assumed that no individual will receive more than one transmission intervention (testing, PPE, vaccination) within a single day, and K-12 children cannot be vaccinated. Finally, because children are commonly asymptomatic, recovered K-12 key contacts are not considered, i.e., for $j \in \{S_1, S_2\}$, $x_{jkR}^i = 0$.

2.3 Representing Normalcy

One objective of CC19LP is to permit the study of the balance between the expected rate of fatalities and the level of normalcy. Normal activity levels are represented by the highest levels defined in the previous section, namely S_2, W_2, and A_5. To encourage normalcy, weights on occupations and activity levels are specified as below, where higher weight is closer to normal and closer to zero is more restrictive.

$a_{S_1} = 0.01$ $a_{W_0} = 0$ $a_{A_1} = 0$ $a_{A_4} = 0.015$
$a_{S_2} = 0.02$ $a_{W_1} = 0.01$ $a_{A_2} = 0.005$ $a_{A_5} = 0.02$
$a_{W_2} = 0.02$ $a_{A_3} = 0.01$

The combined normalcy weight for individuals in occupation j with activity level k is:

$a_j + a_k$, where $j \in \{S_1, S_2, W_0, W_1, W_2\}, \quad k \in \{A_1, A_2, A_3, A_4, A_5\}$.

The total weight over all key contact individuals is then:

$$\sum_j \sum_k \left\{ (a_j + a_k) \sum_i x_{jk}^i \right\}.$$

The relative values of the weights are what matter, so the total weight is scaled between the range of 0 to 10, where 0 mimics an environment closest to rigorous compliance of precautions, and 10 mimics pre-pandemic normal activity.

2.4 Expected Fatality Rate

The primary objective is the expected number of fatalities per day. For a given assignment of key contacts to activity levels (x_{jk}^i), this objective is calculated by first counting (per day) fatalities for both key contacts (Group 2) and associated sheltered high-risk individuals (Group 1) that would occur *without* any transmission interventions of COVID-19 testing, PPE, or vaccination. However, recovered key contact individuals benefit from a protection factor γ_V that for now is assumed to be the same as vaccination, and K-12 school children benefit from a transmission reduction factor $\gamma_S < 1$. Next, given the assignment of transmission interventions (x_{jkT}^i, x_{jkM}^i, x_{jkV}^i), the counts for those *saved* are subtracted from the objective. This allows an examination of the effectiveness of transmission interventions.

The probability of fatality for an individual is based on the law of total probability, as follows:

P(fatality) = P(fatality | infection) P(infection | contact) P(contact),

where a contact is a close contact with a contagious individual with the virus. The fatality rate replaces the probability of contacts with a rate of contacts. Different average contact rates were specified in Section 3 for every occupation $j \in \{S_1, S_2, W_0, W_1, W_2\}$ and every community activity level $k \in \{A_1, A_2, A_3, A_4, A_5\}$. Denote these rates as ρ_C^j and ρ_C^k, respectively. Assume the rates of contacts for different occupations and activities are independent, then key contact individuals in occupation j at activity level k have average close contact rates of $\rho_C^j + \rho_C^k$ with other individuals. If the probability that a contact is contagious is p^+, then the contact rates with contagious individuals are $\rho_{C+}^j + \rho_{C+}^k = p^+(\rho_C^j + \rho_C^k)$. Estimates for p^+ are unknown, so CC19LP uses reported cases, a ratio of unknown to known cases [37-38], and average contagious periods for unknown (4.5 days) and known (10 days) [39-42]. Specific calculations are discussed in the Appendix.

To calculate the infection rate, let $p^H_{I|C+}$ be the transmission probability (probability of infection) for high-risk individuals when in close contact with a contagious individual, and let $p^L_{I|C+}$ be the corresponding transmission probability for low-risk individuals. It is possible for $p^H_{I|C+} > p^L_{I|C+}$, if high-risk individuals are more susceptible to infection. The rate of infection for high-risk key contacts in occupation *j* with activity level *k* is $(p^H_{I|C+})(\rho^j_{C+} + \rho^k_{C+})$, and similarly for low-risk key contacts. Finally, to calculate the fatality rate, let $p^H_{F|I}$ and $p^L_{F|I}$ be the probability of fatality, given infected, for high-risk and low-risk individuals, respectively, where $p^H_{F|I} > p^L_{F|I}$. The fatalities among key contacts (Group 2) without testing, PPE, and vaccine interventions can now be calculated as follows:

$$
\begin{aligned}
E[\text{Fatalities}] = \Bigg\{ & p^H_{F|I}(p^H_{I|C+})(p^+) \sum_j \sum_k (\rho^j_C + \rho^k_C)\,(x^{H_1}_{jk} + x^{H_2}_{jk} - \gamma_V(x^{H_1}_{jkR} + x^{H_2}_{jkR})) \\
& + p^L_{F|I}(p^L_{I|C+})(p^+) \sum_k \Bigg\{ \gamma_S \sum_{j\in\{S_1,S_2\}} \left(\rho^j_C + \rho^k_C\right)(x^{L_1}_{jk}) \\
& + \sum_{j\in\{W_0,W_1,W_2\}} \left(\rho^j_C + \rho^k_C\right)(x^{L_1}_{jk} + x^{L_2}_{jk} - \gamma_V(x^{L_1}_{jkR})) \Bigg\} \Bigg\}. \qquad (1)
\end{aligned}
$$

The fatalities among sheltered high-risk individuals (Group 1) depend on close contacts with their associated key contact individual. If this key contact individual is infected, then the sheltered high-risk individual will be at risk for infection. To capture this, let ρ^0_C be the average close contact rate per day for sheltered high-risk individuals with their associated key contact individual. Then the rate of infection for a sheltered high-risk individual associated with a low-risk key contact is $(p^H_{I|C+})(\rho^0_C)(p^L_{I|C+})(\rho^j_{C+} + \rho^k_{C+})$, where the last two terms in the product give the rate of infection for low-risk key contacts in occupation *j* and activity level *k*, and the first two terms give the rate of infection for sheltered high-risk individuals by contagious key contacts. To capture the multiple fatalities that may be associated with key contacts, let μ_H be the mean number of sheltered high-risk individuals for each high-risk key contact individual, and let μ_L be the corresponding mean for each low-risk key contact individual. Since all low-risk key contacts must be associated with sheltered high-risk individuals, $\mu_L \geq 1$. Since high-risk key contacts need not have associated high-risk individuals, $\mu_H \leq \mu_L$. The means μ_L and μ_H are calibrated to match the number of sheltered high-risk individuals (Group 1), leading to their fatalities without transmission interventions:

$$E[\text{Fatalities}] = p_{F|I}^{H}(p_{I|C+}^{H})\rho_C^0 \Bigg\{ \mu_H(p_{I|C+}^{H})(p^+) \sum_j \sum_k \left(\rho_C^j + \rho_C^k\right)\left(x_{jk}^{H_1} + x_{jk}^{H_2} - \gamma_V(x_{jkR}^{H_1} + x_{jkR}^{H_2})\right)$$
$$+ \mu_L(p_{I|C+}^{L})(p^+) \sum_j \sum_k \left(\rho_C^j + \rho_C^k\right)\left(x_{jk}^{L_1} - \gamma_V(x_{jkR}^{L_1})\right) \Bigg\}. \quad (2)$$

If an individual is wearing high-grade PPE, such as an N95 mask, let γ_M be the protection factor reducing transmission. Assuming PPE interventions are highly effective, γ_M should be very high, nominally 0.95. The probability of transmission when wearing PPE drops to $(1-\gamma_M)p_{I|C+}^{H}$ for a high-risk individual. However, compliance is an issue with wearing PPE, so CC19LP defines p_M^i as the probability of a type *i* individual complying with wearing high-grade PPE, where those living in a crowding environment have lower compliance probabilities. The count of all key contact individuals (Group 2) saved by PPE, shown in equation (3), is similar to equation (1), using the probability of being saved from infection with the PPE intervention decision variables:

$$E[\text{Saved}] = \gamma_M \Bigg\{ p_{F|I}^{H}(p_{I|C+}^{H})(p^+) \sum_j \sum_k (\rho_C^j + \rho_C^k)\left(p_M^{H_1} x_{jkM}^{H_1} + p_M^{H_2} x_{jkM}^{H_2}\right)$$
$$+ p_{F|I}^{L}(p_{I|C+}^{L})(p^+) \sum_K \Bigg\{ \gamma_S \sum_{j\in\{S_1,S_2\}} \left(\rho_C^j + \rho_C^k\right)(p_M^{L_1} x_{jkM}^{L_1})$$
$$+ \sum_{j\in\{W_0,W_1,W_2\}} \left(\rho_C^j + \rho_C^k\right)(p_M^{L_1} x_{jkM}^{L_1}) \Bigg\} \Bigg\}. \quad (3)$$

Similar to equation (2), the count of sheltered high-risk individuals (Group 1) that are saved by their associated key contacts wearing PPE can be written as:

$$E[\text{Saved}] = p_{F|I}^{H}\gamma_M(p_{I|C+}^{H})(\rho_C^0) \Bigg\{ \mu_H(p_{I|C+}^{H})(p^+) \sum_j \sum_k \left(\rho_C^j + \rho_C^k\right)\left(p_M^{H_1} x_{jkM}^{H_1} + p_M^{H_2} x_{jkM}^{H_2}\right)$$
$$+ \mu_L(p_{I|C+}^{L})(p^+) \sum_j \sum_k \left(\rho_C^j + \rho_C^k\right)\left(p_M^{L_1} x_{jkM}^{L_1}\right) \Bigg\}. \quad (4)$$

For COVID-19 testing interventions, the key contact can still become infected, so the benefit is to quarantine the key contact, so that associated high-risk individuals do not risk infection. In particular, consistent testing of the key contact may catch infection before symptoms arise or if the key contact remains asymptomatic. Some additional probabilities are

needed to represent uncertainty in test results and quarantine compliance. Let p_T^+ be the probability of an infected and contagious individual testing positive, and let $p_{Q|T}^i$ be the probability of a type i individual complying with quarantine after testing positive. Assume $p_{Q|T}^i < p_{Q|T}^{i'}$, where $i = H_2$ and $i' \in \{H_1, L_1\}$. The count for those sheltered high-risk individuals (Group 1) saved by testing their associated key contacts, shown in equation (5), is again similar to equation (2) with the additional probabilities due to testing:

$$E[\text{Saved}] = p_{F|I}^H (p_{I|C+}^H)(\rho_C^0)(p_T^+) \left\{ \mu_H (p_{I|C+}^H)(p^+) \sum_j \sum_k \left(\rho_C^j + \rho_C^k\right) \left(p_{Q|T}^{H_1} x_{jkT}^{H_1} + p_{Q|T}^{H_2} x_{jkT}^{H_2}\right) \right.$$
$$\left. + \mu_L (p_{I|C+}^L)(p^+) \sum_j \sum_k \left(\rho_C^j + \rho_C^k\right) \left(p_{Q|T}^{L_1} x_{jkT}^{L_1}\right) \right\}. \quad (5)$$

If an individual is vaccinated, the calculation of fatalities is similar to equations (3) and (4) for PPE. Equation (6) below counts key contact individuals (Group 2) saved due to vaccination:

$$E[\text{Saved}] = \gamma_V \left\{ p_{F|I}^H (p_{I|C+}^H)(p^+) \sum_j \sum_k (\rho_C^j + \rho_C^k) \left(x_{jkV}^{H_1} + x_{jkV}^{H_2}\right) \right.$$
$$+ p_{F|I}^L (p_{I|C+}^L)(p^+) \sum_K \left\{ \gamma_S \sum_{j \in \{S_1, S_2\}} \left(\rho_C^j + \rho_C^k\right)\left(x_{jkV}^{L_1}\right) \right.$$
$$\left. \left. + \sum_{j \in \{W_0, W_1, W_2\}} \left(\rho_C^j + \rho_C^k\right)\left(x_{jkV}^{L_1}\right) \right\} \right\}. \quad (6)$$

Equation (7) below counts sheltered high-risk individuals (Group 1) saved due to vaccinating their associated key contacts:

$$E[\text{Saved}] = p_{F|I}^H \gamma_V (p_{I|C+}^H)(\rho_C^0) \left\{ \mu_H (p_{I|C+}^H)(p^+) \sum_j \sum_k \left(\rho_C^j + \rho_C^k\right) \left(x_{jkV}^{H_1} + x_{jkV}^{H_2}\right) \right.$$
$$\left. + \mu_L (p_{I|C+}^L)(p^+) \sum_j \sum_k \left(\rho_C^j + \rho_C^k\right) \left(x_{jkV}^{L_1}\right) \right\}. \quad (7)$$

To handle vaccinated sheltered high-risk individuals (Group 1), the means μ_H and μ_L are adjusted downward using the vaccination protection factor γ_M with the vaccinated proportion,

resulting in fewer fatalities among sheltered high-risk individuals (Group 1) calculated in equation (2).

Finally, the expected fatalities per day is the sum of the fatalities in equations (1) and (2) minus those saved in equations (3) though (7). It should be noted that p^+ is a scalar multiplier throughout the calculation, which means the *optimal* CC19LP interventions do *not* depend on this uncertain value. This is a benefit from directly employing an optimization to study interventions rather than using predictive models or simulation models that are popular in public health. However, having a reasonably accurate estimate of the expected daily fatality rate is still important in practice. As a guideline, decision-makers can identify a low daily average of reported fatalities that was realized by that county. The allowable normalcy level could be selected based on maintaining a CC19LP expected daily fatality rate near this realistic guideline.

2.5 Objectives and Constraints

The two conflicting objectives are:

(1) Minimizing the expected daily fatality rate derived in Section 5.

(2) Attaining a desired level of normalcy, as represented in Section 4.

CC19LP directly minimizes fatalities and constrains normalcy as follows:

$$\sum_j \sum_k \left\{ (a_j + a_k) \sum_i x_{jk}^i \right\} \geq B,$$

where B is a lower limit on normalcy. In the 0-10 scale, 10 corresponds to the maximum possible value of B. To maintain mass balance of key contact individuals for each risk type $i \in \{L_1, H_1, H_2\}$, let N^i be the number of key contact individuals, with N_S^i counting the K-12 children and N_W^i counting adults, and define the following equality constraints:

$$\sum_k (x_{S_1 k}^i + x_{S_2 k}^i) = N_S^i,$$

$$\sum_k (x_{W_0 k}^i + x_{W_1 k}^i + x_{W_{2k}}^i) = N_W^i,$$

$$\sum_j \sum_k x_{jk}^i = N^i.$$

Similarly, given the fraction f_R^i of recovered key contacts of each risk type i, the mass balance constraint on the number of adult key contacts that are recovered is:

$$f_R^i N_W^i = \sum_{j \in \{W_0, W_1, W_2\}} \sum_k x_{jkR}^i .$$

Resource constraints on daily testing and PPE are:

$$\sum_i \sum_j \sum_k x_{jkT}^i \le N_T \ , \qquad \sum_i \sum_j \sum_k x_{jkM}^i \le N_M \ ,$$

where N_T is the upper limit on the number of key contacts that can be tested per day, and N_M is the upper limit on the number of key contacts that can be protected daily by high-grade PPE. For vaccine interventions only full vaccination protection is considered. For some vaccines, full protection is attained a couple weeks after the completion of 2 doses. An individual that has received only one dose of a 2-dose regimen is not considered vaccinated in CC19LP. Because vaccinated individuals remain vaccinated in the future, consider a planning time horizon of N_D days over which interventions are to be optimized. Let f_V^i be the fraction of key contacts of risk type *i* that were already fully protected by vaccination prior to the planning time horizon, and let N_V be the maximum number of key contacts that can be vaccinated over these N_D days. Then the number of fully protected vaccinated adult key contacts during the planning horizon must be at least the number that were already vaccinated:

$$f_V^i N_W^i \le \sum_{j \in \{W_0, W_1, W_2\}} \sum_k x_{jkV}^i \ .$$

and the upper limit on the cumulative number of fully protected vaccinated adult key contacts is:

$$\sum_i \sum_j \sum_k x_{jkV}^i \le N_V + \sum_i f_V^i \, N_W^i \ .$$

Finally, each key contact can either be recovered or receive at most one transmission intervention:

$$0 \le x_{jkR}^i + x_{jkT}^i + x_{jkM}^i + x_{jkV}^i \le x_{jk}^i \ ,$$
$$0 \le x_{jk}^i, x_{jkR}^i, x_{jkT}^i, x_{jkM}^i, x_{jkV}^i \ .$$

For the activity level fractions defined in Section 3, the following constraints are defined. First, some K-12 key contact children may not be able to properly comply with social precautions at school, and consequently there could be a lower limit on those that must participate at the S_2 level:

$$f_{S_2}^i N_S^i \le \sum_k x_{S_2 k}^i \le N_S^i \ .$$

For key contact adults, there is an upper limit on the number of each risk type *i* that can work online, and a lower limit on those that cannot comply with social precautions at work:

$$0 \le \sum_k x^i_{W_0 k} \le f^i_{W_0} N^i_W \,,$$
$$f^i_{W_2} N^i_W \le \sum_k x^i_{W_2 k} \le N^i_W \,.$$

For the community activity levels, these constraints define upper limits on key contacts attaining the lower A_1 and A_2 levels:

$$0 \le \sum_j x^i_{jA_1} \le f^i_{A_1} N^i \,,$$
$$0 \le \sum_j \left(x^i_{jA_1} + x^i_{jA_2}\right) \le \left(f^i_{A_1} + f^i_{A_2}\right) N^i,$$

and these constraints define lower limits on key contacts attaining the higher A_4 and A_5 levels:

$$f^i_{A_5} N^i \le \sum_j x^i_{jA_5} \le N^i \,,$$
$$\left(f^i_{A_4} + f^i_{A_5}\right) N^i \le \sum_j \left(x^i_{jA_4} + x^i_{jA_5}\right) \le N^i.$$

These last two constraints are important for specifying the crowding environment for key contacts of risk type H_2, where a large proportion maintain high community activity levels. Key contacts not subject to crowding may have unconstrained activity levels.

3 Case Studies

An online version of CC19LP was awarded a third place prize in the C3.ai COVID-19 Grand Challenge (https://c3.ai/c3-ai-covid-19-grand-challenge/), and can be accessed from the COSMOS COVID-19 project site (https://cosmos.uta.edu/projects/covid-19/). The online tool was tested for all 3,142 U.S. county areas, including the District of Columbia. Table 1 presents CC19LP input parameter settings that were assumed for all counties. County-specific input parameter settings are discussed in the Appendix. County-level 2018 Census data and CDC risk-factor data from the 2018 BRFSS Survey are used to conduct key contact partitioning, shown in Table 2 for ten metropolitan counties. The fraction of 2-or-more-person households with persons 0-17, combined with the fraction of children aged 5-17, is used to count K-12 key contacts. This partitioning is an estimate, given that the designation of a key contact depends on household dynamics that are not specified in publicly available data. In general, these estimate over 50% of the population as baseline low-risk individuals (Group 3), which includes most children. Further, the sheltered high-risk population (Group 1) is only about 10% of the population, which implies that most high-risk individuals cannot isolate and are included as key contact individuals (Group 2). About 30% of the total population are high-risk key contacts, and it is these individuals that should be provided higher protection in public and prioritized for vaccination.

Benchmarking was first conducted for the ten metropolitan counties for Spring/Summer 2020 time periods following major lockdowns across the U.S. to reduce case counts. This is early in the pandemic when PPE was not rigorously employed. The COVID-19 testing rate was about one test per thousand population per day [49-50]. To estimate p^+ (probability of a contagious individual), actual case counts [49-50] and various ratios of unknown cases to known reported cases are studied [37-38]. Table 3 compares the actual average daily fatalities to the CC19LP estimates under different ratios. The closest match is seen for a 4:1 (80% unknown) or 3:1 (75% unknown) ratio for most counties, but Tarrant's closest match is between 5:1 (83.33% unknown) and 4:1, and Philadelphia's closest match is between 3:1 and 2:1 (66.67% unknown). Tarrant is in Texas, which reopened very quickly following the mandated lockdown, and Philadelphia is in Pennsylvania, which was the slowest state to reopen, so the inferred ratios make logical sense. The minimum normalcy was assumed for the key contact group in each county, shown in the bottom row of Table 3. A normalcy of zero is not attainable due to the constraints on activity levels. CC19LP normalcy only pertains to key contact individuals (Group 2), and the minimum normalcy assumes key contacts are doing their best to properly attain CDC social precautions, subject to the constraints. Baseline low-risk individuals (Group 3) could engage in higher activity levels, which are represented in the actual reported case counts.

A Fall 2020 time period was then selected to further study Miami-Dade County in Florida. By fall, health care and public safety workers (HC&PS) had access to high-grade PPE, and the national rate of testing was about 2.75 per thousand population per day. To benchmark this time period, minimum normalcy is still assumed for key contacts, but CC19LP optimal PPE allocations are constrained to cover HC&PS workers, and it is assumed that other key contacts were not provided easy access to high-grade PPE. Recovered individuals were estimated based on U.S. numbers, with reported cases and fatalities comprising approximately 2% and 0.06% of the U.S. population, respectively. In Table 4, benchmarking results employing high-grade PPE only for HC&PS (12.48) are comparable to the actual average daily fatalities (11.71). In this solution, 61% of PPE is allocated to low-risk HC&PS workers. Without the constraint on HC&PS, CC19LP optimal interventions shift high-grade PPE away from HC&PS workers of risk types L_1 and H_1 and toward key contacts of risk type H_2. The expected daily fatality rate drops to 6.28, which implies that about 6 lives could have been saved *per day* in Miami-Dade County if high-grade PPE had been made available to these more vulnerable H_2 key contacts.

Next, a hypothetical Winter 2021 Miami-Dade study with vaccination was conducted to study the effectiveness of the different transmission interventions. Recovered individuals were again estimated based on U.S. numbers, with reported cases and fatalities comprising approximately 6.8% and 0.1% of the U.S. population, respectively. Optimal PPE is allocated with supply maintained as in Fall 2020, and nationwide testing was nearly 5.0 per thousand population per day. Benchmarking was not conducted since data on vaccinated populations partitioned by risk factors was not available. Instead, we assume no prior key contacts are fully vaccinated and set a rate of 5.0 individuals fully vaccinated per day. A breakdown of the CC19LP expected daily fatalities calculation (Section 5) is presented in Table 5 for a Normalcy of 4 on the 0-10 scale. The impact of PPE is still seen to save the most lives, and testing has little impact. By contrast, vaccination, at the same 5.0 daily rate as testing, clearly has a measurable

impact. Although PPE saves 4 times more lives than vaccination, the daily PPE usage rate is over 10 times the rate of vaccination, demonstrating the effectiveness of vaccination over PPE.

Figure 2 displays the corresponding Winter 2021 CC19LP optimal allocation of interventions. Specifically, it is seen that key contacts may participate at the highest levels of activity (W_2 and/or A_4 or A_5), if they are allocated PPE or vaccination, and vaccines are prioritized for the H_2 key contact group, which is primarily composed of those key contacts living in crowding environments. Further, daily COVID-19 testing was allocated to low-risk key contacts because it is less risky for them to become ill, but by quarantining positive cases, their associated sheltered high-risk individuals could be protected. However, as previously mentioned, testing in general has little impact on preventing fatalities. The reason why those living with crowding were not allocated tests is because their quarantine compliance was assumed to be lower.

Finally, a hypothetical run was conducted to study the impact if all key contacts could be vaccinated, using Winter 2021 PPE supply, testing rate, and recovered individuals. If we assume the reported case counts from January 11-31, 2021, then the prevalence of the virus in the community is too high to enable higher levels of Normalcy. However, if we assume the reported case counts from September 10-30, 2020, then it is seen in Table 6 that a low fatality rate can be achieved with higher Normalcy. Reported case counts in March 2021 are similar to those in October 2020 and are approaching the September 2020 counts [49]. Consequently, if counties can prioritize their efforts on vaccinating CC19LP key contact individuals, which overall comprise about 35-40% of the population (see Table 2), then a return to Normalcy may begin prior to attaining "herd immunity" of approximately 60-80% vaccinated.

Table 1: CC19LP input parameter settings [43-48].

Description of CC19LP Input Parameter	**Notation**	**Setting**
Transmission probability for high-risk individual	$p^{H}_{I\|C+}$	0.05281
Transmission probability for low-risk individual	$p^{L}_{I\|C+}$	0.02987
Protection factor, if wearing high-grade PPE	γ_M	0.9500
Protection factor, if fully vaccinated	γ_V	0.9000
Probability of L_1 key contact complying with high-grade PPE	$p^{L_1}_{M}$	0.9500
Probability of H_1 key contact complying with high-grade PPE	$p^{H_1}_{M}$	0.9500
Probability of H_2 key contact complying with high-grade PPE	$p^{H_2}_{M}$	0.7500
Probability of a contagious individual testing positive	p^{+}_{T}	0.7000
Probability of L_1 key contact complying quarantine	$p^{L_1}_{Q\|T}$	0.9800
Probability of H_1 key contact complying with quarantine	$p^{H_1}_{Q\|T}$	0.9800
Probability of H_2 key contact complying with quarantine	$p^{H_2}_{Q\|T}$	0.5000
Fatality probability for high-risk individual	$p^{H}_{F\|I}$	0.0800
Fatality probability for low-risk individual	$p^{L}_{F\|I}$	0.0020
Reduction factor for fatality probability for K-12 children	γ_S	0.3765

Table 2: Key contacts composition in percent of the total population for Texas counties Dallas, Harris, and Tarrant; Maricopa County in Arizona; Miami-Dade County in Florida; Los Angeles County in California; Cook County in Illinois; Queens County in New York; Philadelphia County in Pennsylvania; and King County in Washington state.

Key Contact Type	**Dallas**	**Harris**	**Tarrant**	**Maricopa**	**Miami-Dade**
Total County Population	2,586,552	4,602,523	2,019,977	4,253,913	2,715,516
Group-1: Sheltered	8.31%	8.51%	9.06%	10.33%	9.98%
Group-2: Key Contacts	34.71%	34.18%	34.80%	37.17%	39.85%
Group-3: Baseline	56.98%	57.32%	56.14%	52.50%	50.16%
K-12-Children	0.48%	0.50%	0.48%	0.50%	0.82%
L_1 Low-risk Adult	3.54%	3.62%	3.62%	3.89%	4.94%
H_1 High-risk Adult	25.95%	25.44%	26.70%	28.03%	26.83%
H_2 High-risk Adult	4.75%	4.61%	4.00%	4.74%	7.27%
Key Contact Type	**Los Angeles**	**Cook**	**Queens**	**Philadelphia**	**King**
Total County Population	10,098,052	5,223,719	2,298,513	1,575,522	2,163,257
Group-1: Sheltered	9.55%	8.85%	9.88%	8.90%	8.83%
Group-2: Key Contacts	34.81%	38.85%	38.27%	40.30%	38.32%
Group-3: Baseline	55.63%	52.30%	51.85%	50.80%	52.85%
K-12-Children	0.66%	0.56%	0.77%	0.54%	0.42%
L_1 Low-risk Adult	4.75%	4.47%	5.95%	5.36%	3.94%
H_1 High-risk Adult	24.24%	28.31%	26.27%	26.02%	30.18%
H_2 High-risk Adult	5.16%	5.52%	5.28%	8.37%	3.78%

Table 3: Actual average daily fatalities vs. CC19LP during Spring/Summer 2020. CC19LP estimates in boldface are closest to actual average daily fatalities.

	Dallas	**Harris**	**Tarrant**	**Maricopa**	**Los Angeles**
Fatality Period	May 1–31	Jun 1–15	May 1–31	May 25–Jun 3	May 19–Jun 7
Avg. Daily Fatalities	**4.16**	**6.47**	**3.13**	**8.20**	**35.00**
3-week Prior Period	Apr 10–30	May 11–31	Apr 10–30	Apr 25–May 15	Apr 28–May 18
Reported Cases	2,028	4,100	1,495	3,705	17,500
CC19LP (5:1 ratio)	4.89	9.59	**3.29**	9.14	43.12
CC19LP (4:1 ratio)	**3.97**	7.79	2.67	**7.43**	**35.04**
CC19LP (3:1 ratio)	3.05	**6.00**	2.06	5.71	26.95
CC19LP (2:1 ratio)	2.14	4.20	1.44	4.00	18.87
Minimum Normalcy	2.79	2.78	2.70	2.75	2.83
	Miami-Dade	**Cook**	**Queens**	**Philadelphia**	**King**
Fatality Period	Jun 1–30	Jun 23–Jul 13	Jun 5–29	Jul 5–31	Jun 12–30
Avg. Daily Fatalities	**9.63**	**14.29**	**12.00**	**3.70**	**1.26**
3-week Prior Period	May 11–31	Jun 2–22	May 11–31	Jun 13–Jul 3	May 22–Jun 11
Reported Cases	3,800	7,700	5,113	1,800	900
CC19LP (5:1 ratio)	12.23	21.03	13.74	6.62	2.01
CC19LP (4:1 ratio)	**9.93**	17.09	**11.16**	5.38	1.64
CC19LP (3:1 ratio)	7.64	**13.14**	8.59	**4.14**	**1.26**
CC19LP (2:1 ratio)	5.35	9.20	6.01	2.90	0.88
Minimum Normalcy	2.97	2.81	2.90	3.20	2.69

Table 4: Actual vs. CC19LP for Fall 2020 with a PPE supply sufficient for healthcare and public safety (HC&PS) workers and recovered individuals.

	Miami-Dade
Sep. 10–30 Reported Cases	7,506
Oct. 1–31 Avg. Daily Fatalities	**11.71**
Testing per 1000 per day (U.S. rate)	2.75
PPE per 1000 per day (HC&PS supply)	54
Full Vaccination per 1000 per day	0
CC19LP with HC&PS PPE allocation (4:1 ratio)	**12.48**
PPE allocation: 61% L_1, 32% H_1, 7% H_2	
CC19LP Optimal PPE allocation (4:1 ratio)	**6.28**
PPE allocation: 0% L_1, 4% H_1, 96% H_2	

Table 5: Breakdown of CC19LP expected daily fatalities calculation for a hypothetical Winter 2021 scenario with a PPE supply sufficient for healthcare and public safety (HC&PS) workers and recovered individuals as of January 31, 2021.

	Miami-Dade
Jan 11–31 Reported Cases	43,400
Testing per 1000 per day (U.S. rate)	5
PPE per 1000 per day (HC&PS supply)	54
Full Vaccination per 1000 per day	5
CC19LP Expected Daily Fatalities Calculation	
Fatalities (No Transmission Interventions)	55.92
Lives Saved with Testing	**0.66**
Lives Saved with PPE	**24.34**
Lives Saved with Vaccination	**6.55**
CC19LP Estimate (4:1 ratio)	24.37
CC19LP Normalcy	4

Table 6: Hypothetical scenario using Fall 2020 reported cases with a PPE supply sufficient for healthcare and public safety (HC&PS) workers, full vaccination available for all key contacts, and recovered individuals as of January 31, 2021.

	Miami-Dade
Sep. 10–30 Reported Cases	7,506
Testing per 1000 per day (U.S. rate)	5
PPE per 1000 per day (HC&PS supply)	54
Full Vaccination per 1000 per day	400
CC19LP Reopening Comparison	
CC19LP Normalcy for key contacts (minimum)	2.97
CC19LP Optimal PPE allocation (4:1 ratio)	**1.9945**
CC19LP Normalcy for key contacts	4.00
CC19LP Optimal PPE allocation (4:1 ratio)	**2.1227**
CC19LP Normalcy for key contacts	5.00
CC19LP Optimal PPE allocation (4:1 ratio)	**3.1977**

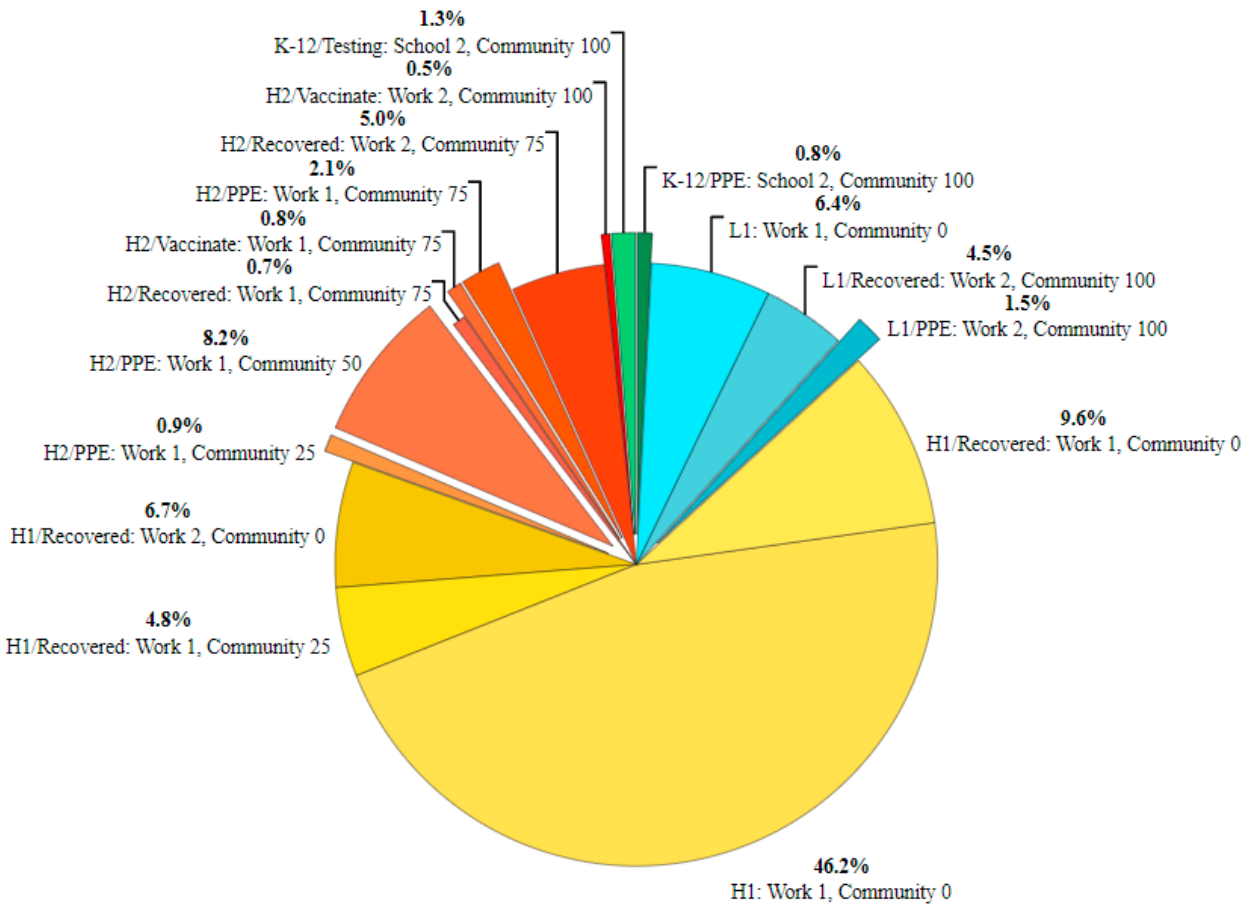

Figure 2: CC19LP optimal allocations for the Miami-Dade Winter 2021 case in Table 5. Green = K-12 children. Blue = Low-risk adults (L_1). Yellow = High-risk without crowding (H_1). Orange = High-risk living with crowding (H_2). See Section 3 for notation on activity levels. Slices are sorted clockwise from lowest risk (K-12) to highest risk (H_2) and sorted within risk type by activity levels (Work, Community). Pulled-out pie slices indicate controlled transmission interventions using COVID-19 testing, high-grade PPE, or full vaccination.

4 Concluding Remarks

CC19LP demonstrates the effectiveness of an aggregate and computationally fast optimization approach in both matching reality and identifying interventions that simultaneously save the most lives while balancing reopening. A key element of the CC19LP framework is identifying key contact individuals. High-risk individuals that are protected in the framework can be identified by age or by medical experts. Sheltered high-risk individuals should isolate and identify associated key contacts. High-risk individuals that cannot isolate, due to work or other occupations, are key contacts. Low-risk individuals may be classified as key contacts if they are associated with sheltered high-risk individuals or require close contact with high-risk individuals at their occupation, such as in health care. To accommodate key contacts, some businesses implemented concessions, such as protective barriers for employees, special grocery store hours for the high-risk population, restaurant take-out with minimal contact, and personnel scheduling [51-54]. However, key contacts have not been sufficiently recognized in communities. As an example, a wedding in Maine on August 7, 2020 led to an outbreak and 7 deaths [55], and none of the fatalities were wedding attendees. Consequently, all fatalities were due to transmission from wedding attendees that would have been classified as key contacts in the CC19LP framework. If key contacts had properly maintained social precautions or been provided high-grade PPE at the wedding, then this outbreak and subsequent fatalities could have been averted.

As seen in Figure 2, CC19LP optimal interventions allocate high-grade PPE to high-risk key contacts and testing to low-risk key contacts. Use of PPE to protect high-risk frontline workers fits with the CC19LP optimal solution, but CC19LP solutions extend the use of PPE to protect high-risk key contact individuals living with crowding, such as nursing home residents and low-income communities. U.S. policies for COVID-19 testing focused on testing those with symptoms. This is contrary to CC19LP, which recommends testing low-risk key contacts that can quarantine, so as to protect their associated sheltered high-risk individuals. However, when testing became more available, policies encouraged more testing to detect asymptomatic and pre-symptomatic cases among low-risk individuals. Regardless, it was seen in Table 5 that testing has very little impact on saving lives. Finally, results in Table 6 provide hope that reopening could be possible before the vaccination effort reaches “herd immunity” if CC19LP key contacts are prioritized for vaccination. As mentioned in Sections 2 and 7, a questionnaire to identify CC19LP key contacts and a CC19LP webtool are freely available online. Additional CC19LP results, including key contacts for all U.S. counties, Fall 2020 runs, and a Summer 2021 run for the entire U.S., can be found on the same COSMOS COVID-19 project website.

Acknowledgment: The authors thank Norman H. Edelman, M.D. for sharing his perspective on the COVID-19 pandemic. Dr. Edelman is Professor of Medicine; Core Faculty, Program in Public Health. Stony Brook University. In addition, these individuals assisted with running CC19LP to obtain the presented results: Kara Annis, Mohammad Al Saed, and Shubhasheesh Dwivedi.

References:

1. De Serres, G., I. Rouleau, M. E. Hamelin, C. Quach, D. Skowronski, L. Flamand, N. Boulianne, L. Yan, J. Carbonneau, A.-M. Bourgault, M. Couillard, H. Charest, and G. Boivin. (2010). Contagious period for pandemic (H1N1) 2009. *Emerging infectious diseases*, **16(5)**, 783–788.
2. Wei, W. E., Z. Li, C. J. Chiew, S. E. Yong, M. P. Toh, and V. J. Lee (2020). Presymptomatic Transmission of SARS-CoV-2—Singapore, January 23–March 16, 2020. *Morbidity and Mortality Weekly Report*, **69(14)**, 411.
3. Hu, Z., C. Song, C. Xu, G. Jin, Y. Chen, X. Xu, H. Ma, W. Chen, Y. Lin, Y. Zheng, J. Wang, Z. Hu, and H. Shen (2020). Clinical characteristics of 24 asymptomatic infections with COVID-19 screened among close contacts in Nanjing, China. *Science China Life Sciences*, **63(5)**, 706-711.
4. Rothe, C., M. Schunk, P. Sothmann, G. Bretzel, G. Froeschl, C. Wallrauch, C., T. Zimmer, V. Thiel, C. Janke, W. Guggemos, M. Seilmaier, C. Drosten, P. Vollmar, K. Zwirglmaier, S. Zange, R. Wölfel, and M. Hoelscher (2020). Transmission of 2019-nCoV infection from an asymptomatic contact in Germany. *New England Journal of Medicine*, **382(10)**, 970-971.
5. Mizumoto, K., K. Kagaya, A. Zarebski, and G. Chowell (2020). Estimating the asymptomatic proportion of coronavirus disease 2019 (COVID-19) cases on board the Diamond Princess cruise ship, Yokohama, Japan, 2020. *Eurosurveillance*, **25(10)**, 2000180.
6. Bendavid, E., B. Mulaney, N. Sood, S. Shah, E. Ling, R. Bromley-Dulfano, D. Tversky, C. Lai, Z. Weissberg, R. Saavedra-Walker, J. Tedrow, D. Tversky, A. Bogan, T. Kupiec, D. Eichner, R. Gupta, J. Ioannidis, J. Bhattacharya (2020). COVID-19 Antibody Seroprevalence in Santa Clara County, California. *medRxiv*, DOI: 10.1101/2020.04.14.20062463.
7. Adhikari, S. P., Meng, S., Wu, Y. J., Mao, Y. P., Ye, R. X., Wang, Q. Z., ... & Zhou, H. (2020). Epidemiology, causes, clinical manifestation and diagnosis, prevention and control of coronavirus disease (COVID-19) during the early outbreak period: a scoping review. *Infectious Diseases of Poverty*, **9(1)**, 1-12.
8. Wilder-Smith, A. and D. P. Freedman (2020). Isolation, quarantine, social distancing and community containment: pivotal role for old-style public health measures in the novel coronavirus (2019-nCoV) outbreak. *Journal of Travel Medicine*, **27(2)**, DOI: 10.1093/jtm/taaa020.
9. Salathé, M., C. L. Althaus, R. Neher, S. Stringhini, E. Hodcroft, J. Fellay, M. Zwahlen, G. Senti, M. Battegay, A. Wilder-Smith, I. Eckerle, M. Egger, and N. Low (2020). COVID-19 epidemic in Switzerland: on the importance of testing, contact tracing and isolation. *Swiss Medical Weekly*, **150**, DOI: 10.4414/smw.2020.20225.
10. Lee, V. J., C. J. Chiew, and W. X. Khong (2020). Interrupting transmission of COVID-19: lessons from containment efforts in Singapore. *Journal of Travel Medicine*, DOI: 10.1093/jtm/taaa039.

11. Joseph, A. (2020). Contact tracing could help avoid another lockdown. Can it work in the U.S.?, https://www.statnews.com/2020/05/29/contact-tracing-can-it-help-avoid-more-lockdowns/, accessed on June 3, 2020.
12. Moore, R. C., Lee, A., Hancock, J. T., Halley, M., & Linos, E. (2020). Experience with Social Distancing Early in the COVID-19 Pandemic in the United States: Implications for Public Health Messaging. *medRxiv*, DOI: 10.1101/2020.04.08.20057067.
13. Wu, Z. and J. M. McGoogan. (2020). Characteristics of and important lessons from the coronavirus disease 2019 (COVID-19) outbreak in China: summary of a report of 72 314 cases from the Chinese Center for Disease Control and Prevention. *JAMA*, **323(13)**, 1239-1242.
14. Wang, X., Z. Du, G. Huang, S. Fox, and L. A. Meyers (2020). COVID-19 in Austin, Texas: Relaxing Social Distancing Measures. *The University of Texas at Austin COVID-19 Modeling Consortium*, https://sites.cns.utexas.edu/sites/default/files/cid/files/austin_relaxing_social_distancing.pdf?m=1587681780, accessed on May 3, 2020.
15. van Bunnik, B. A. D., A. L. K. Morgan, P. R. Bessell, G. Calder-Gerver, F. Zhang, S. Haynes, J. Ashworth, S. Zhao, N. R. Cave, M. R. Perry, H. C. Lepper, L. Lu, P. Kellam, A. Sheikh, G. F. Medley, and M. E. J. Woolhouse (2020). Segmentation and shielding of the most vulnerable members of the population as elements of an exit strategy from COVID-19 lockdown, https://www.wiki.ed.ac.uk/display/Epigroup/COVID-19+project, accessed on May 7, 2020.
16. Ferrier, G. D. and C. K. Lovell (1990). Measuring cost efficiency in banking: Econometric and linear programming evidence. *Journal of Econometrics*, **46(1-2)**, 229-245.
17. Chen, M. and W. Wang (1997). A linear programming model for integrated steel production and distribution planning. *International Journal of Operations & Production Management*, **17(6)**, 19.
18. van Zon, A. H. and G. J. Kommer (1999). Patient flows and optimal health-care resource allocation at the macro-level: a dynamic linear programming approach. *Health Care Management Science*, **2(2)**, 87-96.
19. Barnes, E. R., V. C. P. Chen, B. Gopalakrishnan, and E. L. Johnson (2002). "A Least Squares Primal-Dual Algorithm for Solving Linear Programming Problems." *Operations Research Letters*, **30(5)**, 289–294.
20. Chen, V. C. P., D. Günther, and E. L. Johnson (2003). "Solving for an Optimal Airline Yield Management Policy via Statistical Learning." *Journal of the Royal Statistical Society, Series C*, **52 Part 1**, 1–12.
21. Earnshaw, S. R., K. Hicks, A. Richter, and A. Honeycutt (2007). A linear programming model for allocating HIV prevention funds with state agencies: a pilot study. *Health Care Management Science*, **10(3)**, 239-252.
22. P. Phananiramai, J. M. Rosenberger, V. C. P. Chen, S. B. Kim, and M. L. Sattler (2011). A mathematical optimization technique for managing selective catalytic reduction for coal-fired power plants. *Energy Systems*, **2**, 171-188.

23. G. Saito, H. W. Corley, J. M. Rosenberger, T.-K. Sung, and A. Noroziroshan (2015). Constraint optimal selection techniques (COSTs) for nonnegative linear programming problems. *Applied Mathematics and Computation*, **251**, 586-598.
24. Fallahi, A., J. M. Rosenberger, V. C. P. Chen, W.-J. Lee, and S. Wang (2019). "Linear programming for multi-agent demand response." *IEEE Access*, **7**, 181479-181490.
25. Lindsley, W. G., J. D. Noti, F. M. Blachere, J. V. Szalajda, and D. H. Beezhold (2014). Efficacy of Face Shields Against Cough Aerosol Droplets from a Cough Simulator. *Journal of Occupational and Environmental Hygiene*, **11(8)**, pp. 509-518.
26. Aydin, O., B. Emon, S. Cheng, L. Hong, L. P. Chamorro, and M. T. A. Saif (2020). Performance of fabrics for home-made masks against the spread of COVID-19 through droplets: A quantitative mechanistic study. *Extreme Mechanics Letters*, **40**, 100924.
27. Ueki, H., Y. Furusawa, K. Iwatsuki-Horimoto, M. Imai, H. Kabata, H. Nishimura, and Y. Kawaoka (2020). Effectiveness of face masks in preventing airborne transmission of SARS-CoV-2. *mSphere*, **5(5)**, e00637-20.
28. Stehlé J., N. Voirin, A. Barrat, C. Cattuto, V. Colizza, L. Isella, C. Régis, J.-F. Pinton, N. Khanafer, W. Van den Broeck, and P. Vanhems (2011). Simulation of an SEIR infectious disease model on the dynamic contact network of conference attendees. *BMC* medicine, **9(1)**, 87.
29. Zhan, C, K. T. Chi, Y. Fu, Z. Lai, H. Zhang (2020). Modeling and prediction of the 2019 coronavirus disease spreading in China incorporating human migration data. *medRxiv*, DOI: 10.1101/2020.02.18.20024570.
30. Tatpudi, H., R. Das, and T. K. Das (2020). Impact assessment of full and partial stay-at-home orders, face mask usage, and contact tracing: An agent-based simulation study of COVID-19 for an urban region. *Global Epidemiology*, DOI: 10.1016/j.gloepi.2020.100036.
31. Lee, B. Y., S. T. Brown, P. Cooley, M. A. Potter, W. D. Wheaton, R. E. Voorhees, S. Stebbins, J. J. Grefenstette, S. M. Zimmer, R. Zimmerman, T.-M. Assi, R. R. Bailey, D. K. Wagener, PhD, and D. S. Burke (2010). Simulating School Closure Strategies to Mitigate an Influenza Epidemic. *Journal of Public Health Management and Practice*, **16(3)**, 252–261.
32. Cooley, P., S. Brown, J. Cajka, B. Chasteen, L. Ganapathi, J. Grefenstette, J., C. R. Hollingsworth, B. Y. Lee, B. Levine, W. D. Wheaton, and W. K. Wagener (2011). The role of subway travel in an influenza epidemic: A New York City simulation. *Journal of Urban Health,* **88(5)**, 982.
33. Ghasemi, Y. and Y. Zhou (2018). Agent-Based Modeling for Campus-Specific Transmission of Infectious Diseases. In *Proceedings of the Institute of Industrial and Systems Engineers Conference*, Orlando, FL, May.
34. Best, R. and J. Boice (2021). Where The Latest COVID-19 Models Think We're Headed — And Why They Disagree, https://projects.fivethirtyeight.com/covid-forecasts/, accessed on March 3, 2021.

35. Davis, B. (2018). Put Your Oxygen Mask on First, https://cipherhealth.com/put-your-oxygen-mask-on-first/, accessed on May 5, 2020.
36. Richards, E. (2020). 'Historic academic regression': Why homeschooling is so hard amid school closures, https://www.usatoday.com/story/news/education/2020/04/13/coronavirus-online-school-homeschool-betsy-devos/5122539002/, accessed on May 5, 2020.
37. Heneghan, D., J. Brassey, T. Jefferson (2020). COVID-19: What proportion are asymptomatic? https://www.cebm.net/covid-19/covid-19-what-proportion-are-asymptomatic/, accessed on April 29, 2020.
38. Ing, A. J., C. Cocks, and J. P. Green (2020). COVID-19: in the footsteps of Ernest Shackleton. *Thorax*, **75**, pp. 693–694.
39. Gillespie, C (2020). COVID-19: How long after having Coronavirus are you contagious? Here's what doctors say, https://www.health.com/condition/infectious-diseases/coronavirus/how-long-after-coronavirus-are-you-contagious, accessed on July 3, 2020.
40. Housen, T., A. E. Parry, M. Sheel (2020). How long are you infectious when you have coronavirus? https://theconversation.com/how-long-are-you-infectious-when-you-have-coronavirus-135295, accessed on May 5, 2020.
41. Nikolai, L. A., C. G. Meyer, P. G. Kremsner, and T. P. Velavan (2020). Asymptomatic SARS Coronavirus 2 infection: Invisible yet invincible. *International Journal of Infectious Diseases*, **100**, pp. 112–116.
42. Yang, R, X. Gui, and Y. Xiong (2020). Comparison of Clinical Characteristics of Patients with Asymptomatic vs. Symptomatic Coronavirus Disease 2019 in Wuhan, China. *JAMA Network Open*, **3(5)**, e2010182.
43. Du, Z., X. Wang, R. Pasco, M. Petty, S. J. Fox, L. A. Meyers (2020). COVID-19 healthcare demand projections: 22 Texas cities, https://sites.cns.utexas.edu/sites/default/files/cid/files/covid-19_analysis_for_22_texas_cities_033020.pdf?m=1585596798, accessed on April 29, 2020.
44. Verity, R., L. C. Okell, I. Dorigatti, P. Winskill, C. Whittaker, N. Imai, G. Cuomo-Dannenburg, H. Thompson, P. G. T. Walker, H. Fu, A. Dighe, J. T. Griffin, M. Baguelin, S. Bhatia, A. Boonyasiri, A. Cori, Z. Cucunubá, R. FitzJohn, K. Gaythorpe, W. Green, A. Hamlet, W. Hinsley, D. Laydon, G. Nedjati-Gilani, S. Riley, S. van Elsland, E. Volz, H. Wang, Y. Wang, X. Xi, C. A. Donnelly, A. C. Ghani, and N. M. Ferguson (2020). Estimates of the severity of COVID-19 disease, *medRxiv*, DOI: 10.1101/2020.03.09.20033357.
45. Oliver, S. E., J. W. Gargano, M. Marin, M. Wallace, K. G. Curran, M. Chamberland, N. McClung, D. Campos-Outcalt, R. L. Morgan, S. Mbaeyi, J. R. Romero, H. K. Talbot, G. M. Lee, B. P. Bell, and K. Dooling (2020). The Advisory Committee on Immunization Practices' Interim Recommendation for Use of Pfizer-BioNTech COVID-19 Vaccine - United States, December 2020. *Morbidity and Mortality Weekly Report*, **69(50)**, 1922–1924. DOI: 10.15585/mmwr.mm6950e2.

46. Oliver, S. E., J. W. Gargano, M. Marin, M. Wallace, K. G. Curran, M. Chamberland, N. McClung, D. Campos-Outcalt, R. L. Morgan, S. Mbaeyi, J. R. Romero, H. K. Talbot, G. M. Lee, B. P. Bell, and K. Dooling (2021). The Advisory Committee on Immunization Practices' Interim Recommendation for Use of Moderna COVID-19 Vaccine - United States, December 2020. *Morbidity and Mortality Weekly Report*, **69(5152)**, 1653–1656. DOI: 10.15585/mmwr.mm695152e1.
47. Oliver, S. E., J. W. Gargano, H. Scobie, M. Wallace, S. C. Hadler, J. Leung, A. E. Blain, N. McClung, D. Campos-Outcalt, R. L. Morgan, S. Mbaeyi, J. MacNeil, J. R. Romero, H. K. Talbot, G. M. Lee, B. P. Bell, and K. Dooling (2021). The Advisory Committee on Immunization Practices' Interim Recommendation for Use of Janssen COVID-19 Vaccine - United States, February 2021. *Morbidity and Mortality Weekly Report*, **70(9)**, 329–332. DOI: 10.15585/mmwr.mm7009e4.
48. Woloshin, S., N. Patel, and A. S. Kesselheim (2020). False Negative Tests for SARS-CoV-2 Infection - Challenges and Implications. *New England Journal of Medicine*, **383(6)**, e38. DOI 10.1056/NEJMp2015897.
49. Roser, M., H. Ritchie, E. Ortiz-Ospina, and J. Hasell (2020). Coronavirus Pandemic (COVID-19), https://ourworldindata.org/coronavirus, accessed on March 15, 2021.
50. Siebel, T. M. (2020). Enterprise AI Meets COVID-19, https://c3.ai/blog/enterprise-ai-meets-covid-19/, accessed November 15, 2020.
51. Das, A. K. (2020). Protective barriers being installed at supermarket registers, https://www.fox5ny.com/news/protective-barriers-being-installed-at-supermarket-registers, accessed on May 3, 2020.
52. Perper, R. (2020). Here are all the major grocery-store chains around the world running special hours for the elderly and vulnerable to prevent the coronavirus spread, https://www.businessinsider.com/coronavirus-stores-special-hours-elderly-vulnerable-list-2020-3, accessed on May 3, 2020.
53. Bratcher, E. H. (2020). 5 food delivery services with no-contact delivery, https://money.usnews.com/money/personal-finance/articles/food-delivery-services-with-no-contact-delivery, accessed on May 3, 2020.
54. Zucchi, G., M. Iori, and A. Subramanian (2020). Personnel scheduling during COVID-19 pandemic, *Optimization Online*.
55. Mahale, P. C. Rothfuss, S. Bly, M. Kelley, S. Bennett, S. L. Huston, and S. Robinson (2020). Multiple COVID-19 Outbreaks Linked to a Wedding Reception in Rural Maine - August 7–September 14, 2020. *Morbidity and Mortality Weekly Report*, **69(45)**, 1686–1690. DOI: 10.15585/mmwr.mm6945a5.

Appendix

In Section 4, the expected daily fatalities calculation depends on the probability that a contact is contagious (p^+) or, equivalently, the percentage of contagious individuals in the population. CC19LP estimates p^+ based on a 3-week period of reported cases. Table A1 shows the calculations for four of the studied counties, using various ratios of unknown to known cases. These estimates should be viewed as representing the average amount of contagion in the population.

Table A1: Example calculations for contagious individuals for 4 county populations.

Case Counts	**Dallas**	**Maricopa**	**Los Angeles**	**Miami-Dade**
January 11-31, 2021 Reported Cases	**41,300**	**84,300**	**167,100**	**43,400**
Assume 15% do not quarantine	6,195	12,645	25,065	6,510
Unknown Cases				
Assume 4:1 ratio (80% unknown)	165,200	337,200	668,400	173,600
Assume 3:1 ratio (75% unknown)	123,900	252,900	501,300	130,200
Assume 2:1 ratio (66.67% unknown)	82,600	168,600	334,200	86,800
Average Daily # Contagious Individuals				
Known cases contagious 10 days	2,950	6,021	11,936	3,100
Unknown cases (4:1) contagious 4.5 days	35,400	72,257	143,229	37,200
Unknown cases (3:1) contagious 4.5 days	26,550	54,193	107,421	27,900
Unknown cases (2:1) contagious 4.5 days	17,700	36,129	71,614	18,600
Daily # Contagious Individuals				
Under 4:1 ratio (80% unknown)	38,350	78,279	155,164	40,300
Under 3:1 ratio (75% unknown)	29,500	60,214	119,357	31,000
Under 2:1 ratio (66.67% unknown)	20,650	42,150	83,550	21,700
% Contagious Individuals (p+)				
Under 4:1 ratio (80% unknown)	1.48%	1.84%	1.54%	1.48%
	1 out of 67	1 out of 54	1 out of 65	1 out of 67
Under 3:1 ratio (75% unknown)	1.14%	1.42%	1.18%	1.14%
	1 out of 88	1 out of 71	1 out of 85	1 out of 88
Under 2:1 ratio (66.67% unknown)	0.80%	0.99%	0.83%	0.80%
	1 out of 125	1 out of 101	1 out of 121	1 out of 125

Most CC19LP settings for the constraint limits in Section 3 were fixed to the values in Table A2, although they can be varied in the input parameter file. The constraint limits on the higher activity levels for key contacts living in crowding (H_2) depend on the population density and are shown in Table A3. All other constraint limits were unconstrained in the presented case studies.

Table A2: CC19LP fixed constraint limits.

Description of CC19LP Input Parameter	Notation	Setting
Maximum fraction of L_1 key contacts that can work completely online	$f_{W_0}^{L_1}$	0.20
Maximum fraction of H_1 key contacts that can work completely online	$f_{W_0}^{H_1}$	0.20
Maximum fraction of H_2 key contacts that can work completely online	$f_{W_0}^{H_2}$	0
Minimum fraction of L_1 key contacts that cannot comply with social precautions at work	$f_{W_2}^{L_1}$	0.10
Minimum fraction of H_1 key contacts that cannot comply with social precautions at work	$f_{W_2}^{H_1}$	0.10
Minimum fraction of H_2 key contacts that cannot comply with social precautions at work	$f_{W_0}^{H_2}$	0.30
Maximum fraction of H_2 key contacts at activity level A_1	$f_{A_1}^{H_2}$	0
Additional maximum fraction of H_2 key contacts at A_2 or A_1	$f_{A_2}^{H_2}$	0.05

Table A3: Constraint limits on activity levels A_4 and A_5 for key contacts living in crowding (H_2).

Description	Notation	Dallas	Harris	Tarrant	Maricopa	Los Angeles
County square miles		872.80	1,704.40	863.40	9,196.80	4057.1
Population per square mile		2,963.51	2,700.38	2,339.56	462.54	2,488.98
Minimum fraction of H_2 key contacts at activity level A_5	$f_{A_5}^{H_2}$	0.0514	0.0277	0.0519	0.0054	0.0120
Additional minimum fraction of H_2 key contacts at A_4 or A_5	$f_{A_4}^{H_2}$	0.4486	0.4723	0.4481	0.4946	0.4880
Description	**Notation**	**Miami-Dade**	**Cook**	**Queens**	**Philadelphia**	**King**
County square miles		1,898.20	944.70	108.70	134.10	2,115.00
Population per square mile		1,430.57	5,529.50	21,145.47	11,748.86	1,022.82
Minimum fraction of H_2 key contacts at activity level A_5	$f_{A_5}^{H_2}$	0.0250	0.0479	0.2396	0.2136	0.0226
Additional minimum fraction of H_2 key contacts at A_4 or A_5	$f_{A_4}^{H_2}$	0.4750	0.4521	0.2604	0.2864	0.4774